Human contribution to the record-breaking June 2019 heat wave in France

Geert Jan van Oldenborgh, Sjoukje Philip, Sarah Kew (KNMI)
Robert Vautard, Olivier Boucher (IPSL Paris)
Friederike Otto, Karsten Haustein (University of Oxford)
Jean-Michel Soubeyroux, Aurélien Ribes, Yoann Robin (Météo France)
Sonia I. Seneviratne, Martha M. Vogel (ETH Zürich)
Peter Stott (UK Met Office)
Maarten van Aalst (ITC/University of Twente and Red Cross Red Crescent Climate Centre)

Summary

- Every heat wave occuring in Europe today is made more likely and more intense by human-induced climate change. How much more depends very strongly on the event definition: location, season, intensity and duration.
- We use an event definition that focuses on health impacts, the three-day average of daily mean temperature. We considered two spatial scales: the whole of France and one city, Toulouse. We only consider June heat waves because they have a different impact and different trend from heat waves in July and August.
- The observations show a very large increase in the temperature of these heat waves. Currently such an event is estimated to occur with a return period of 30 years, but similarly frequent heat waves would have likely been about 4 ºC cooler a century ago.
- Climate models have systematic biases in representing heat waves at these scales and show smaller trends, more year-on-year variation and fewer really severe heat waves than the observations.
- Combining models and observations we conclude that the heat wave was made *at least* 5 times more likely.
- Heat waves are deadly, although this is not readily visible at the time. This risk is aggravated by climate change, but also by other factors such as an aging population, urbanisation, changing social structures, and levels of preparedness. The full impact is only known after a few weeks when the mortality figures have been analysed. Heat plans have reduced the impact in France and other countries, and are becoming even more important in light of the rising risks.

Introduction, Trigger

A heat wave struck large parts of Europe during the last week of June 2019. The event broke several historical records or June records at single locations in several countries,

including France, Switzerland, Austria, Germany, the Czech Republic, Italy and Spain. In particular, the all-time temperature record for any single station in metropolitan France (old record 44.1°C, Conqueyrac) was broken on June 28 by more than 1.5°C with a new record of 45.9°C, established at Gallargues-le-Montueux near the city of Nîmes. In Switzerland, more than 40 stations experienced record daily maximum temperatures for June on June 26 and 6 high-altitude stations experienced all-time temperature records. A record of 7°C was measured at the 4'810m high Mont Blanc summit. In Austria and the Netherlands, the whole month of June 2019 was the warmest ever recorded, in a large part due to the heat wave. The spatial distribution of the highest 3-day average temperature in June 2019 is shown in Figure 1. It is the largest average over 3 consecutive days for metropolitan France in the month of June, with an anomaly peaking at about 10 degrees relative to the 1981-2010 normal.

In France, extreme heat waves usually occur in mid-summer, when they have less impact on school days and professional activities than in June or September. Due to the heat in June 2019, the government decided to postpone one national school exam, inducing organizational challenges at large scale. In the hottest areas, a number of wildfires took place. In the region of Catalonia in Spain wildfires destroyed several thousands of hectares. In Switzerland, train delays were induced by heat damage to the train tracks. The civil security distributed water to tourists in Rome and in Berlin police cooled city trees with water cannons.

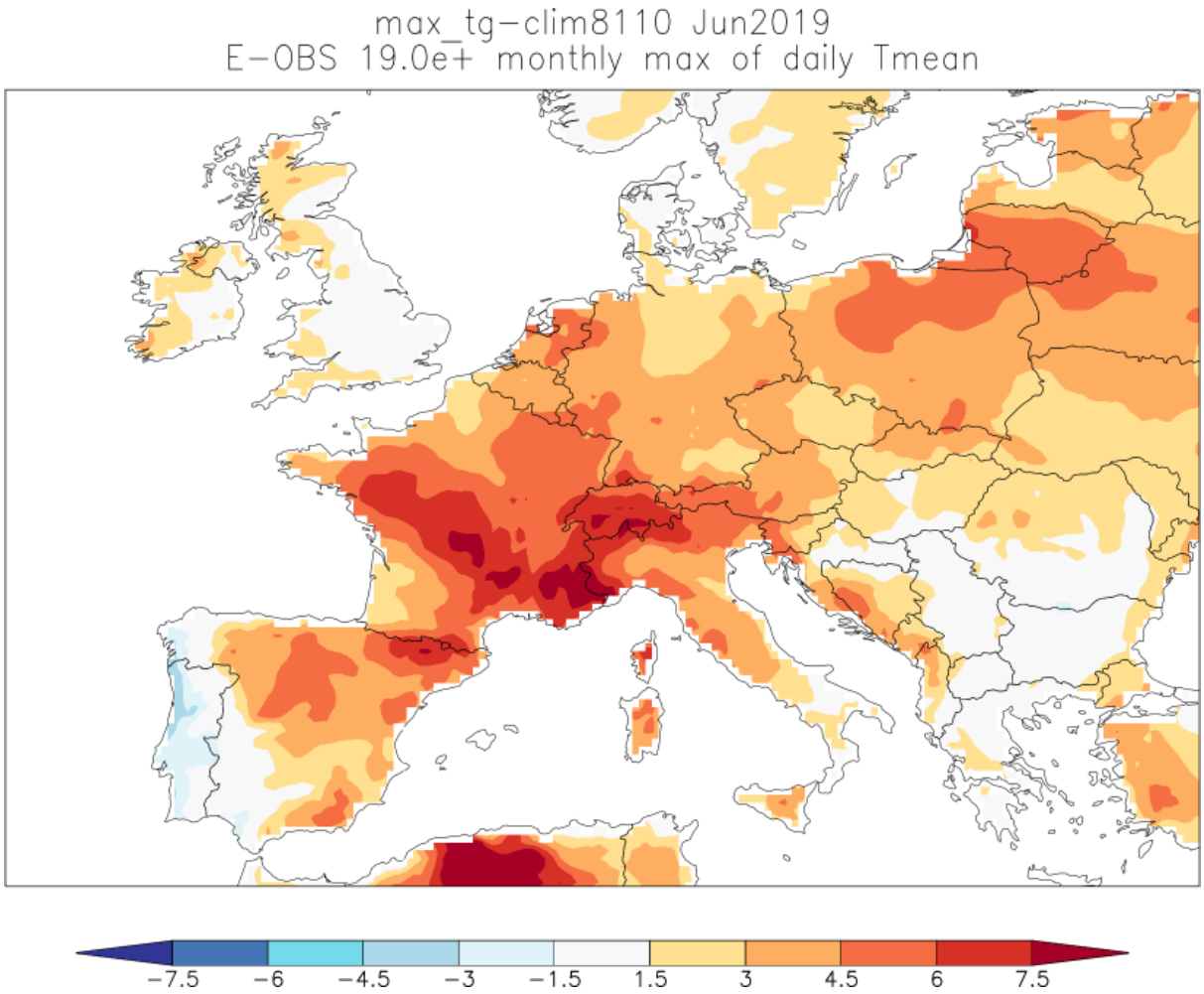

Figure 1a: The highest 3-day daily mean temperature in June 2019 compared to the highest values in 1981–2010 Source: E-OBS (preliminary data)

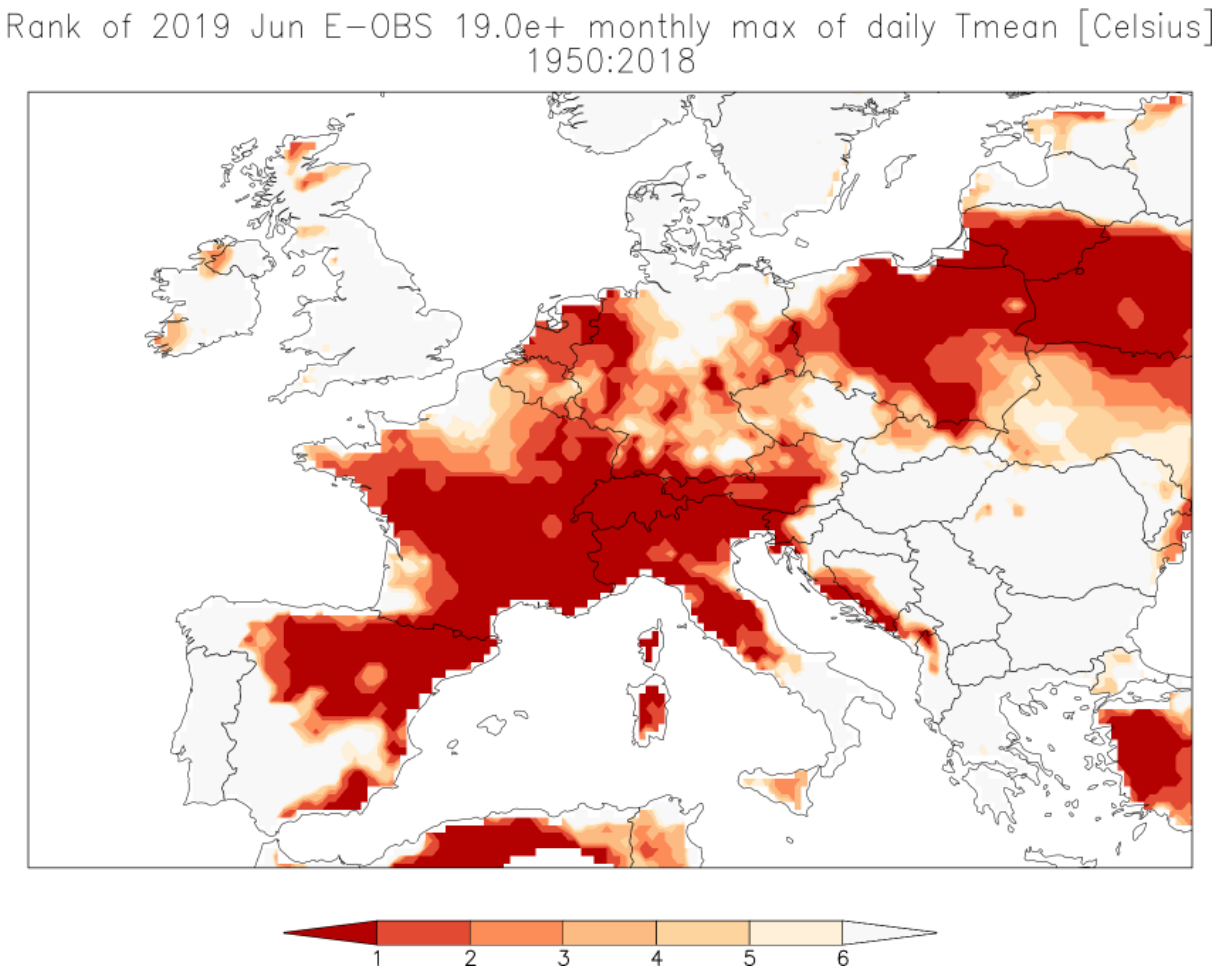

Figure 1b. The rank of the highest 3-day averaged mean temperature in June. Dark red shows where it was the warmest 3-day heat wave in June since 1950, bright red the second-highest etc. Source: E-OBS (preliminary data).

The heat wave occurred rapidly after a rather cool period in the early phase of June. This sudden change was mostly due to the specific dynamical conditions that were present, with a mid-tropospheric "cut-off low" system that formed off the coast of the Iberian peninsula (see the 500 hPa map on 27/6/2019 in Figure 2a). This system created a transport of heat from low-level Saharan air, and induced extreme temperatures at 850 hPa (Figure 2c) and in mountainous areas, such as 29°C at 1600-1800m in the Alps. These dynamical conditions, transporting hot Saharan air or air arising from the Iberian Peninsula are unusual (see analysis below). In particular the fact that the resulting transport of air masses remained at a very low level across the Mediterranean sea over five days was very unusual.

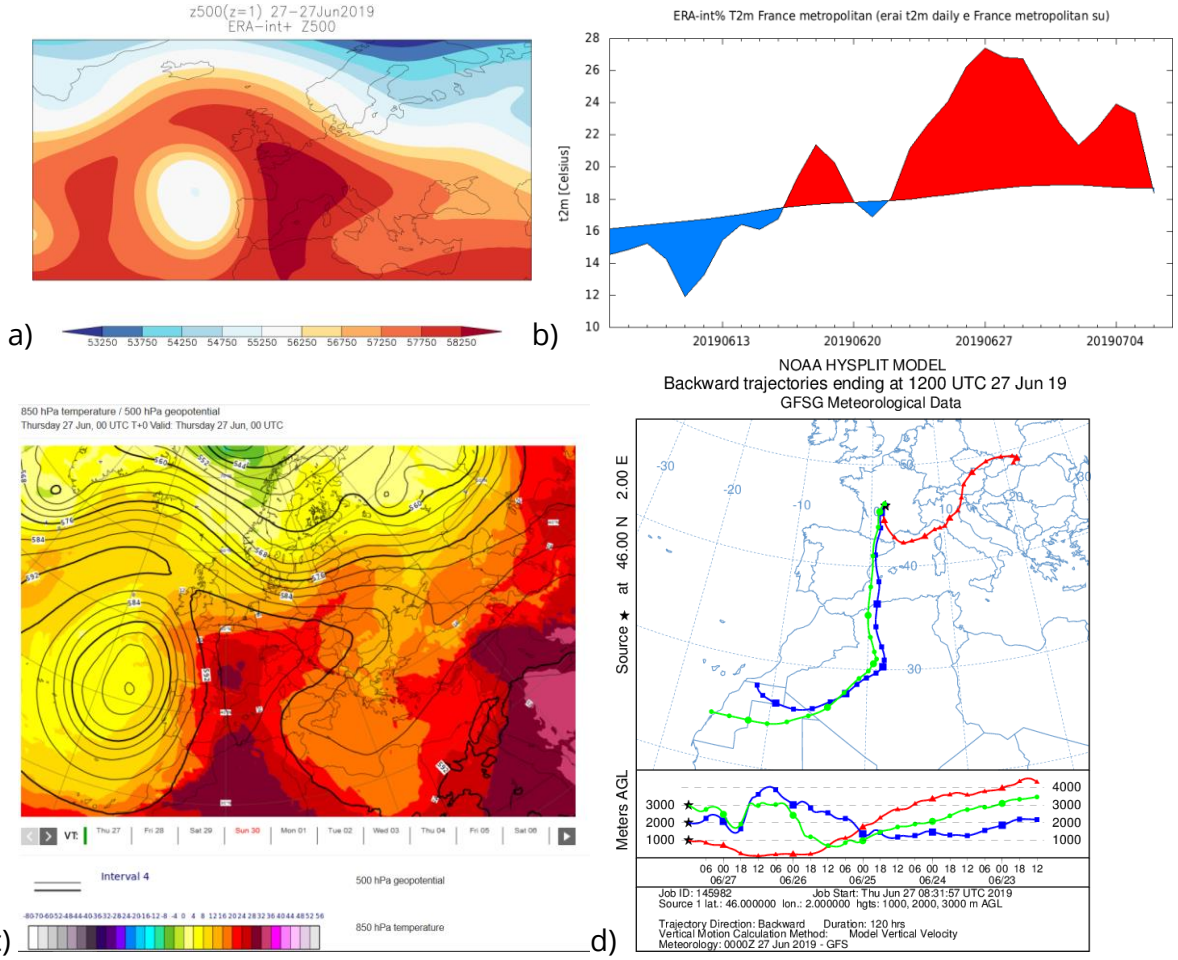

Figure 2: (a) 500 hPa geopotential showing the structure of the flow in the mid troposphere on 27/6/2019. (b) Evolution of the daily temperature averaged over France for a 4-week period around the event. (c)Temperature at 850 hPa and 500 hPa geopotential height from ECMWF analysis (screenshot from http://www.ecmwf.int), showing outstanding values and the northward advection of Saharan air. The upper air origin is confirmed by a back-trajectory analysis using the NOAA HySplit model (d) which represents the 5-day origin of air parcels arriving at 1000m, 2000m and 3000m on 27/6 at 12 UTC on a point in Central France (46°N; 2°E), using the GFS model.

Past heat waves of such magnitude have resulted in significant impacts, in terms of morbidity and mortality, as well as economic damages. Earlier heat waves in the year may have more pronounced impacts on human health given that people have not yet adjusted to the heat over the course of the summer and schools are still in session. If human-induced climate change is making such events more likely, this may have important implications.

Therefore, we investigate how human influence on the climate system has altered the probability and intensity of such an event. While it is well established that human-induced increases in greenhouse gases have *very likely* contributed to increases in hot

extremes across the globe (IPCC 2012, 2013, 2018), we are more generally addressing the question of the actual quantitative assessment of by how much this risk has been increased in the case of the investigated event and locations.

Event definition

We defined the event as the highest 3-day averaged daily mean temperature in June (TG3x). The daily temperature is taken as the average over France and at the city of Toulouse in southern France. These choices were motivated as follows.

The daily mean temperature is as good an indicator of health impacts as the maximum temperature. In the observations it is affected less by local factors such as changing ventilation, as the effects on maximum and minimum temperatures have opposite signs. In models, it is also more robust than the maximum temperature.

Multi-day heat waves have proportionally larger health effects in Europe (D'Ippolita et al, 2010), three days is a length that captures this reasonably well. As mentioned, early season heat waves may have a more severe impact than heat waves in high summer with the same temperature. This is due to the fact that people may not yet have adjusted to the heat, and the holiday season has not yet begun, so people have less opportunity to avoid the highest temperatures. Hence, we only consider June. Health impacts are local, so we took a station in the affected area in Figure 1. Most of the authors happened to be at a conference on extreme events and climate change (IMSC) in Toulouse at the time of the heat wave, Toulouse was forecasted to reach record temperatures and it was close to the region with peak temperatures, so this was a logical choice. We compare the city conditions with the often used average of the metropolitan France measurements (i.e., France without the overseas departments), which has less local influences. This regional average is less relevant for health impacts, but is on the other hand more relevant for electricity demand for cooling, and is often used.

Trend in observations

For the average over France we use the official Météo France definition, which is the average over 30 long-term homogenised stations. Unfortunately, this series is not public but the area average of the E-OBS daily mean temperature over metropolitan France gives virtually identical results. This time series shows previous hot events around 1950, one in 1976, and further ones in 2005 and 2017, in addition to the present event, which set a record for June of 27.5 °C (the 2003 heat wave was more intense but occurred in

August, not June). The 10-yr running mean (green line) shows a combination of the increasing trend due to greenhouse gases and a cooling phase around 1980 mainly due to air pollution (aerosols).

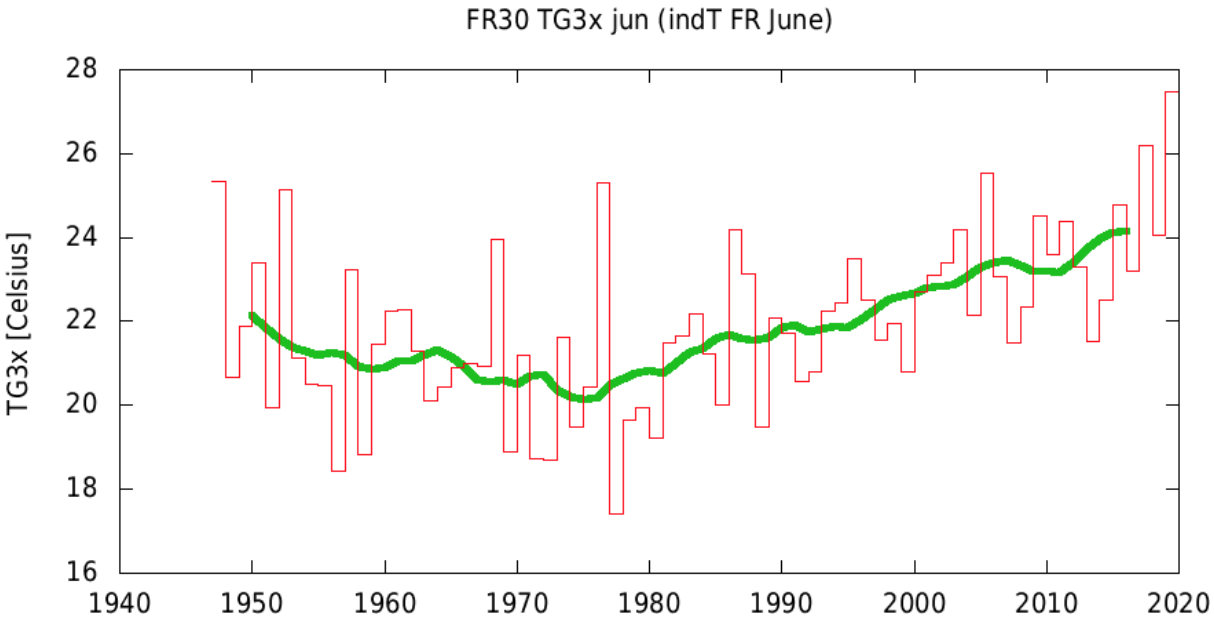

Figure 3. The hottest 3-day mean temperature in the Météo France FR30 France average.

To establish the long-term trend we fit this time series with a covariate that contains a similarly-shaped trend but not the variability. For this series we have to use a time series that contains both the upward trend due to rising global greenhouse gas concentrations and the local cooling period in western Europe around the 1970s. The western European summer (JJA) temperature smoothed with a 15-yr running mean has a similar balance of greenhouse heating and aerosol cooling, see figure 4 (see also van Oldenborgh et al, 2009 and Wild 2009 on effects of aerosols during this time period). For the last years we use fewer years to average. Note that this only prescribes the shape of the time dependence, the amplitude is fitted.

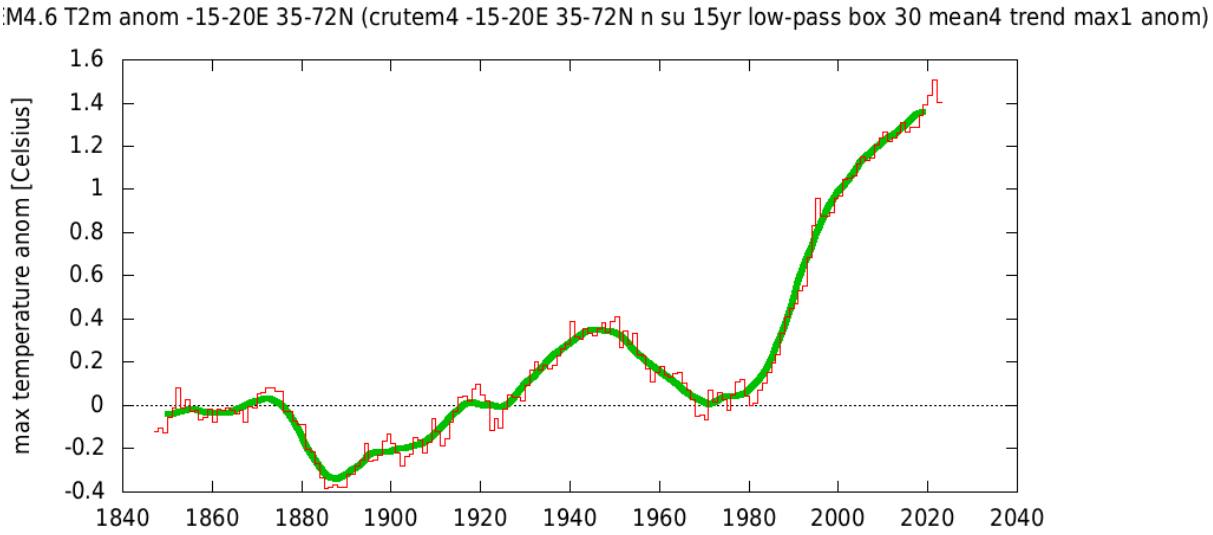

Figure 4. The June–August land temperature (CRUTEM4) averaged over 35-72ºN, 15ºW-20ºE with a 15-yr running mean. The green line denotes an additional 10-yr running mean.

We fit a Generalised Extreme Value distribution (GEV) to the French series (figure 5). The trend is included by allowing for a shift in proportion to the European summer temperature. This gives a good description of 3-day heat in France. We extrapolated the linear relationship found to 1900 to obtain an estimate of the total warming since a time when anthropogenic influences were small (figure 5, left).

This fit (figure 5, right) shows that, taking the greenhouse gas warming and aerosol cooling into account, extreme heat in June as observed in 2019 has a probability of about 3% each year in the current climate (1 in 30 yr), with a 95% uncertainty margin of 0.5% to 7% (1 in 15 to 1 in 200 yr). This is roughly 180 times more than it would have been around 1901 (at least 12 times more). The increase in temperature since 1901 is estimated to be 4.0 °C (3.0 to 5.2 °C) using the scaling of the measured temperature in Toulouse with that of the European temperature average (Figure 4).

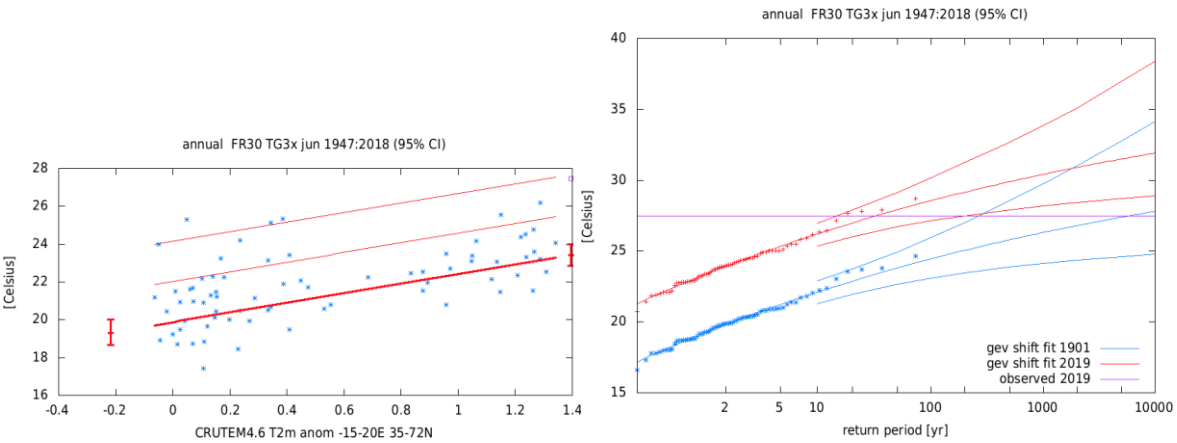

Figure 5: Fit of the highest 3-dy mean daily mean temperature averaged (TG3x) over France in June as a function of 15-yr smoothed European summer temperature in the position parameter of a GEV function. Left: position parameter (thick line) and 6 and 40-yr return times (thin lines) as a function of the smoothed western European land temperature. Right: return period plot with observations and fit drawn for the climates of 1901 and 2019 (observations adjusted with the fitted trend displayed in Figure 4).

This implies a much higher warming trend in France in June compared to that of the average European land summer temperature, which has warmed by about two degrees. More research is needed to understand this feature, but a major factor in the difference is likely the amplification that soil moisture drying contributes to temperature means and extremes in regions with transitional climate between dry and wet conditions. This effect is known to be strong in southern France and other regions with Mediterranean climate and is getting stronger in mid-latitude regions with global warming (because of decreased evaporative cooling if soil moisture levels become limiting for plants' transpiration; e.g. Seneviratne et al, (2010), Mueller and Seneviratne (2012).

Nonetheless, the derived value is particularly high compared to the warming in the European land and could also be affected by additional contributing factors or reflect some shortcomings of the analysis. For instance, the fit was derived from 60 years of data (Figure 5, left) and it is possible that there could be non-linearities in the relationship, e.g., because of a threshold behaviour which could imply a different relationship to European temperatures earlier in the century compared to the derived relationship. In addition, the role of soil moisture feedbacks could be different for means vs extremes, both in France as well as for the European temperatures (since it may also play an amplifying role during extreme conditions in more northern regions). It should be noted that the strength of the feedback may also depend on the month considered (e.g. likely stronger drying at the end of the summer season). Other processes that could also contribute are landscape changes or specific dynamical conditions occurring during hottest extremes in France, which could include hot advections from Spain or Sahara, making the underpinning physical processes different for mean vs extreme cases.

People do not live in large area averages but in single locations, and thus experience heat waves and the impacts on their health locally. As an example of how the probability and intensity of a heat wave like the 2019 one have changed at the local level we chose Toulouse. The 3-day mean of daily mean temperature TG3x was also record high there for June at 30.05 °C. This includes an all-time record daily minimum temperature of 24.2 °C and the highest daily maximum temperature for June, 40.2 °C. The time series of TG3x is shown in figure 5. It follows roughly the same shape as the

average over France, with fewer heat waves around the 1970s and a strong recent increase.

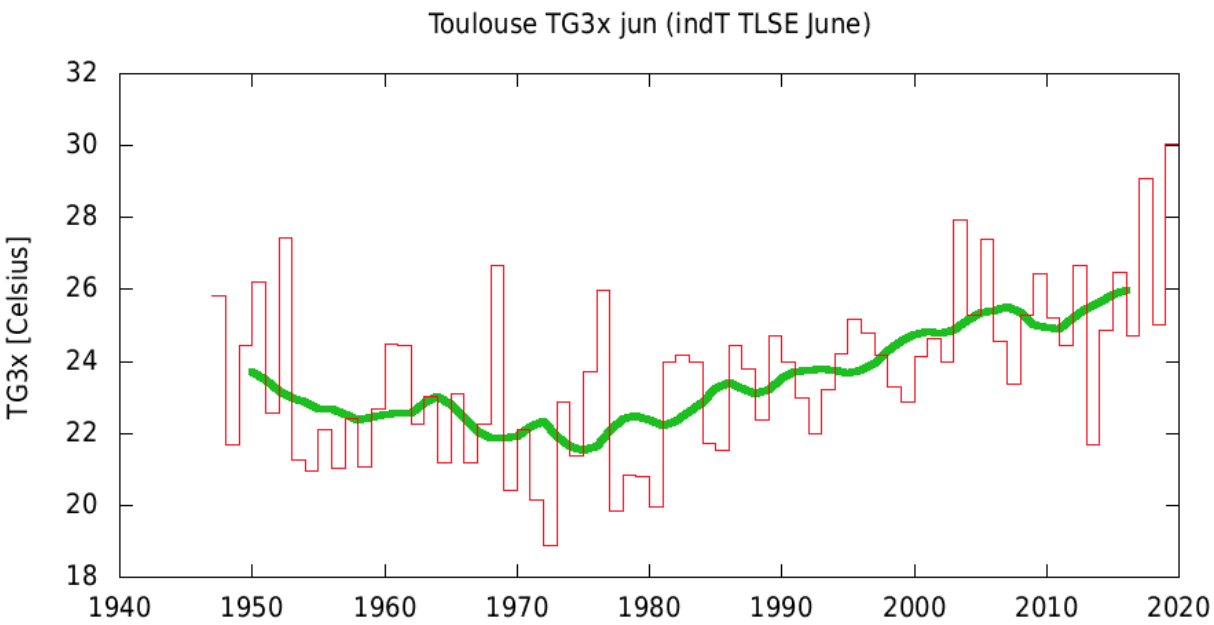

Figure 6. Highest 3-day average daily mean temperature in June at Toulouse. Data: Météo France

The same fit as described above gives a return time in the current climate of 54 yr (16 to 700 yr). This is also around 400 (at least 10) times more likely than it was around 1900. Equivalently, a heat wave defined in this way is now 4.3ºC (2.9 to 6.0 ºC) warmer than it was at the beginning of the last century.

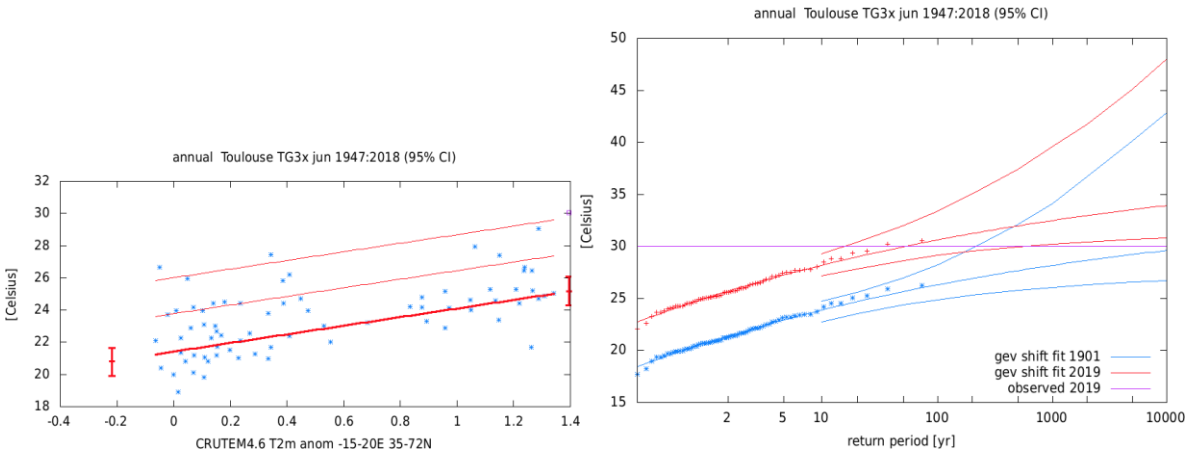

Figure 7: as figure 5 but for Toulouse.

To conclude, the observations of heat waves in France and Toulouse show trends that are very similar in shape to the average summer temperatures, which have been attributed to anthropogenic warming in the more recent part of the time series and

aerosol cooling from the 1950s until about the mid-1980s (Stott et al, 2003, Christidis et al, 2014, Wild 2009). We thus conclude that the increase in probability or intensity is largely due to human-induced climate change.

Before turning to attributing the heat wave defined as June TG3x in the models we analyse whether a trend can be found not only in the temperatures but also in the atmospheric conditions of the observed heat wave. Such a trend would indicate a climate change signal in the dynamical conditions, as suggested by some recent modelling studies.

Dynamics and atmospheric upper-air

Initially we analyse how unusual the atmospheric thermal and dynamical structure in late June 2019 was. The 500 hPa pattern shown in Figure 1a, for the 27th of June 2019, was exceptional in several ways. First, it includes an overall extremely high altitude of the 500 hPa surface, due to the thermal expansion and hot air in the low troposphere (note that this expansion also introduces a trend in the 500 hPa height due to global warming). The average of Figure 3 shows the time series of the June maximum of the 500 hPa height average over Western Europe and the eastern part of the Atlantic (30W-30E; 30N-70N, to encompass the cut-off low). The value is a June record in the NCEP reanalyses series starting in 1948 and such values were obtained only a few times in July or August. No June analogues defined by the Euclidean distance between 500 hPa fields were found for the 27 June cut-off low in the entire time series, due to the very high mean value.

Second, the 500 hPa height pattern (and thereby the wind circulation) is very rare: when considering June analogues calculated with a spatial field correlation, there are 29 “good” analogues, defined as correlated by more than 0.8 with the 27/6 pattern as seen in Figure 2a. This number is very small compared to the usual number of good analogues for usual June patterns: it lies at the 5th percentile of the distribution of the number of good analogues. This result is insensitive to the value of the correlation threshold for defining a good analogue (we have tested 0.7 and 0.6, which provided similar numbers).

Having defined an analogue we have then analysed whether there are significant trends in the number of good analogues or whether there is a larger number of them in the second rather than in the first half of the time series. We do not identify a trend. This analysis thus does not suggest a strong role of climate change in this dynamical aspect of the extreme June heat.

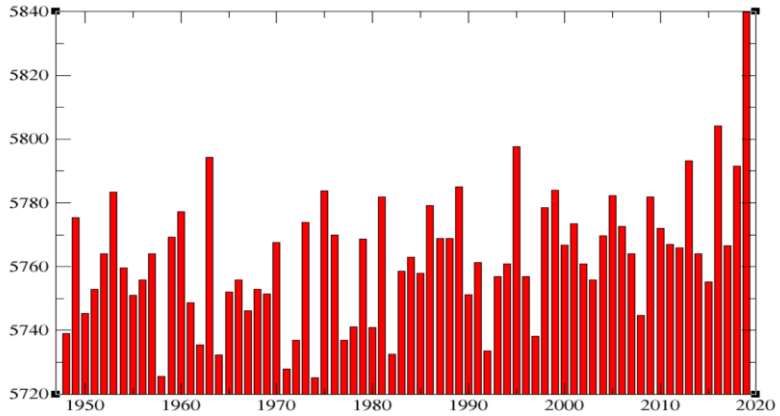

Figure 8: Time series (1949-2019) of the June maximum of daily 500 hPa height averaged over the 30°W-30°E;30°N-70°N region as obtained from NCEP reanalyses.

Model evaluation

Before undertaking the attribution analysis using climate models we have to evaluate whether the models readily available to us are fit for purpose and represent the statistics of the TG3x June event well. We considered the following models to investigate the changes in heat waves in France (Table 1).

Table 1. Overview of models used in this study.

Name	Description	Period	Resolution (atmospheric GCM)
EURO-CORDEX	10 ensemble members of different RCM/GCM combinations, bias-corrected at IPSL. historical/RCP4.5.	1971-2019	11 km
CMIP5	28 simulations from different global climate models which contributed to the 5th phase of the Coupled Modeling Intercomparison Project (CMIP5)	Historical: 1870-2005 RCP8.5: 2005-2100	Between 0.5°x 0.5° to 4°x 4° (between ~50 km and ~400 km)
weather@home	large ensemble of HadRM3P embedded in HadAM3P with prescribed SST, counterfactual 11 different SST patterns subtracted	2006-2015 vs counterfactual 2006-2015	25 km

RACMO 2.2	16 ensemble members downscaling EC-Earth 2.3 historical/RCP8.5 runs	1950-2019	11 km
HadGEM3-A trend	EUCLEIA 15-member ensemble, SST-forced.	1961-2015	N216 (~60 km)
EC-Earth 2.3	16-member ensemble coupled GCM, historical/RCP8.5	1861-2019	T159 (~150 km)
IPSL-CM6A-LR	31-member ensemble coupled GCM, CMIP6 historical (1850-2014) prolonged until 2029 with SSP585 forcing except for constant 2014 tropospheric aerosol forcings	1850-2029	144x142 grid points (~160 km on average)

Further details of these model simulations are given in the Appendix, including key references.

To evaluate these models we test whether the statistics of extreme heat in these models corresponds to the observed statistics. The test consists of fitting the models to the same GEV distribution as in the observations and comparing the scale (σ) and shape (ξ) parameters of the fits to the model data with the parameters of the fits described in the section observational analysis. We do not consider the position parameter (μ) as biases in this parameter can easily corrected without affecting the overall results. We first analyse the results for Metropolitan France (Figs. 8 and 9) and then for Toulouse (Figs. 10 and 11).

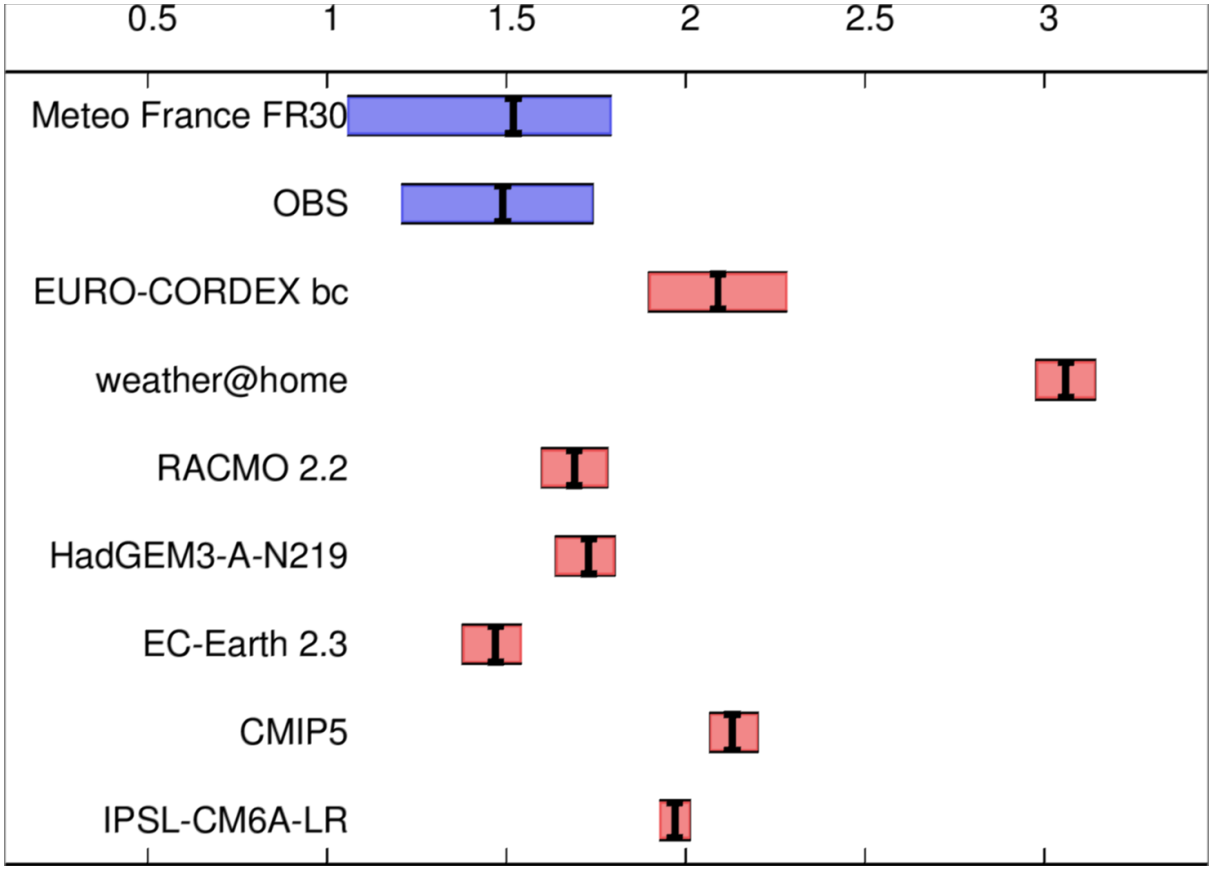

Figure 9: the scale parameter for all models for June TG3x for France.

Figure 9 shows the scale parameter in observations and models for France, which corresponds to the variability of June heat waves from year to year in the country. The EURO-CORDEX and CMIP5 multi-model ensembles and IPSL-CM6A-LR models overestimate this parameter by about 50%, weather@home even by a factor two. If all other parameters would be fixed, this would lead to a negative bias in the probability ratios, as the difference between the cooler climate of the past and the present climate is more within the range of natural variability. Only HadGEM3-A, EC-Earth and the dependent RACMO model would pass a test based on this parameter.

The overall overestimation of heatwave variability in the models for France is likely due to an overestimation of soil moisture-temperature feedbacks in mid-latitude regions, which tends to be a systematic bias of many state-of-the-art climate models (e.g. Sippel et al. 2017).

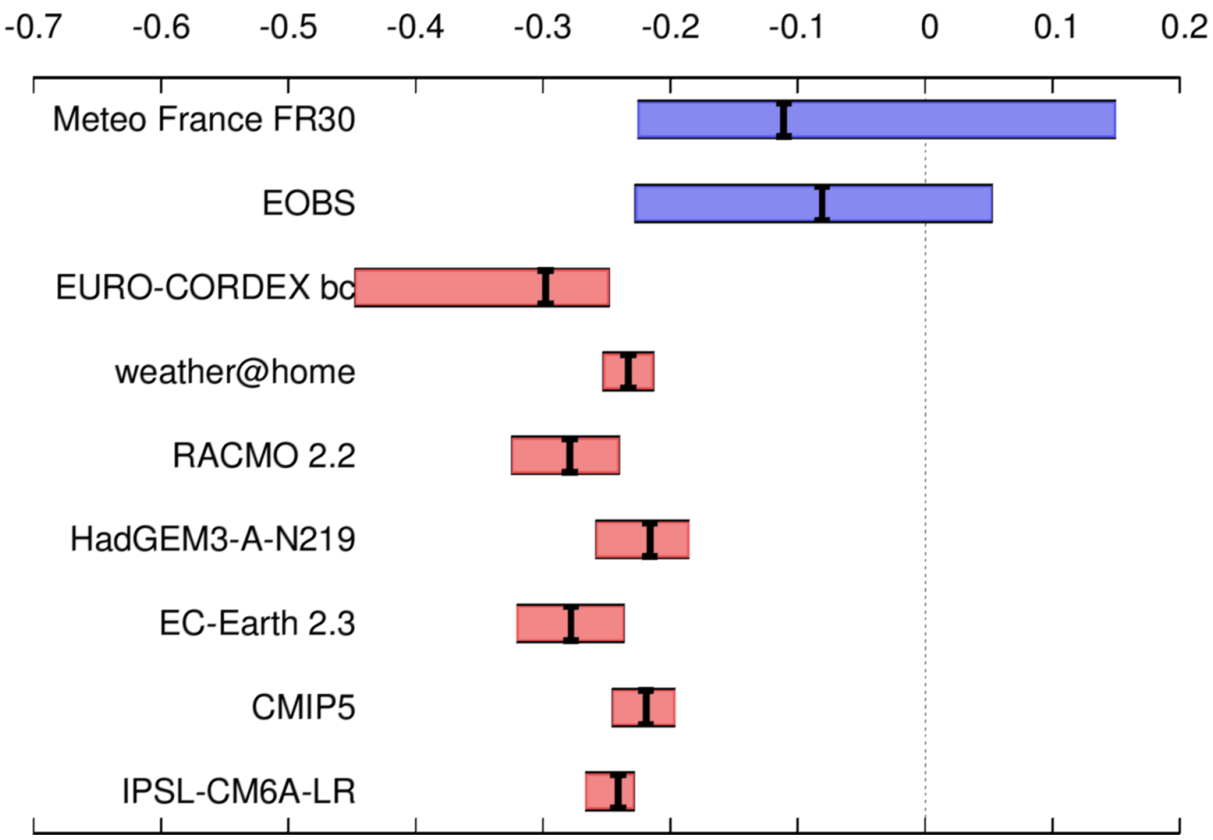

Figure 10: as figure 9 but for the shape parameter.

Figure 10 shows a similar analysis to Figure 9 for the shape parameter in France in June. For heat waves this parameter is generally negative, which implies that for a given climate there is an upper bound to the temperature that can be reached. The upper bound rises with the overall warming though. In France the parameter is less negative than in most regions (Vautard et al, 2018, Fig. 4), possibly because of the soil moisture-temperature feedback (Seneviratne et al. 2010). The models do not seem to be able to reproduce this behaviour and have more negative shape parameters. Too negative a shape parameter will introduce a positive bias in the probability ratio. Formally, the CMIP5 multi-model ensemble, and the weather@home and HadGEM3-A models have uncertainty ranges that overlap with the observations, and would thus pass the test with respect to this parameter whereas the other model simulations or ensembles do not.

Taking the two tests together we find that only one model ensemble or single model (barely) passes the test that the fit parameters of the tail of the distribution have to be compatible with the parameters describing the observations; a situation similar to the one encountered for area-averaged heat waves in the eastern Mediterranean (Kew at al, 2019). A more careful study would also investigate whether the observational analysis did not introduce biases in the fit values for the observations.

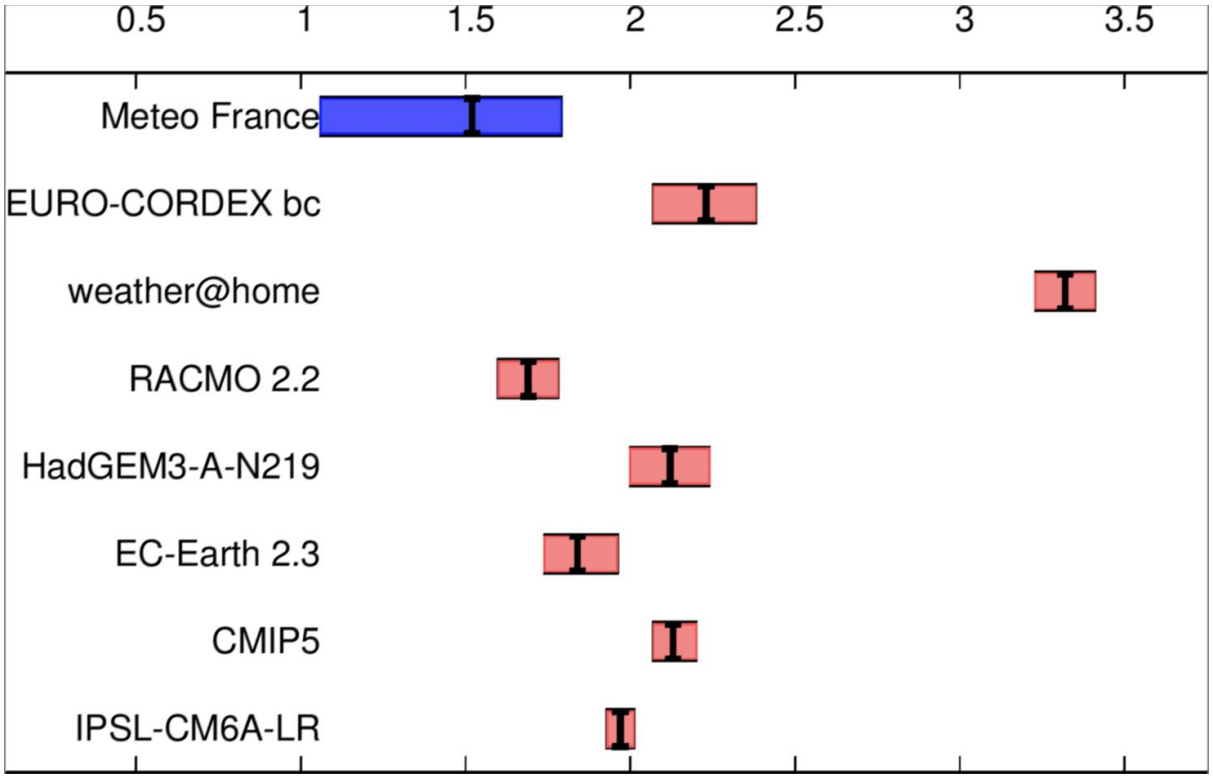

Figure 11: The scale parameter of observations and models compared for the station of Toulouse-Blagnac airport.

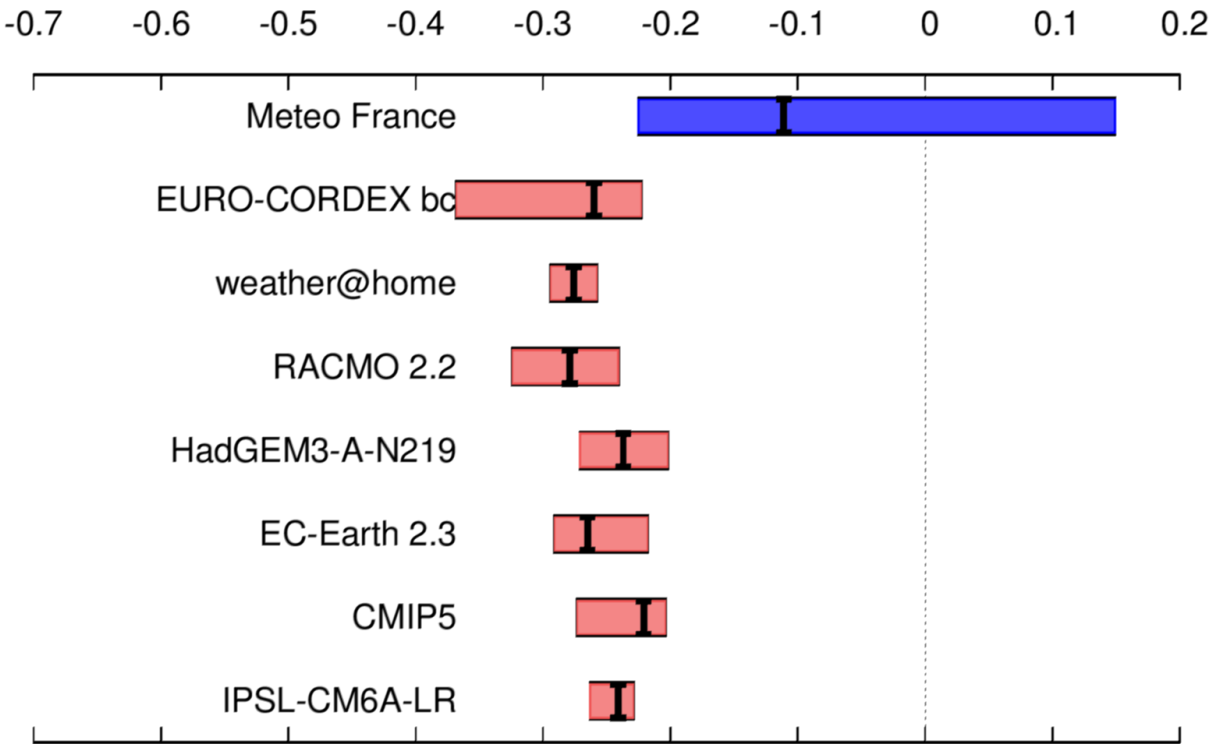

Figure 12. As Figure 11 but for the shape parameter.

For a single station, Toulouse, we find similar results: the two models that do not have an incompatible scale parameter (Figure 11) have incompatible shape parameters (Figure 12), so here no model passes the formal tests. From the analyses for the shape parameter, we see that the CMIP5 multi-model ensemble actually has some overlap with the observations (Fig. 11), however it is outside the range of the observed scale parameters (Fig. 10). Hence, we are formally left for the present analysis with no suitable climate models or model ensembles to do the attribution (though we did not check the suitability of each single CMIP5 models and cannot exclude that some might be suitable for both parameters).

Having thus no well suited models from the analysed sample for the investigated event and locations at this stage, we decide not to give a synthesised overall result drawn from observations and models as in previous studies (refs) but still proceed with analysing all models, noting that the results are only indicative at best when drawing conclusions.

Attribution

For the actual attribution step we use climate model simulations for the same event definition described above and utilising two different methodologies.

One method (EC-Earth, RACMO,HadGEM3-A, CMIP5 ETHZ) treats climate model simulations from transient model runs in the same way as the observations by fitting an extreme value distribution shifted with smoothed European summer temperature from the same model. Strictly speaking this is not a clean attribution methodology as trends in the model, in the same way as in observations, can also have causes other than anthropogenic climate change. However, the only other forcings in these models, volcanoes and variatin in solar activity, have very small effects on these extremes.

The second method (EURO-CORDEX, weather@home, CMIP5 Meteo France, IPSL-CM6A-LR) uses simulations of the present day and compares them with simulations of a counterfactual climate as the present could have been without anthropogenic climate change (weather@home) or simulations of the late 19th century (IPSL-CM6A-LR). The EURO-CORDEX ensemble compares to 1971-2000, the change is next extrapolated to 1900 using the fraction global mean warming realised up to 1985.

It should be noted that the EURO-CORDEX and CMIP5 ensembles are multi-model ensembles. They have been bias-corrected (see Appendix for details) and seem to follow a GEV function well in spite of the different extreme properties of the individual models. However, in the case of the EURO-CORDEX simulations, note that only one

model among the 11 models (the ARPEGE model) include temporally-varying aerosol concentrations.. On the other hand, all CMIP5 GCMs account for temporal variations in aerosol concentrations (Bartok et al. 2017).

For non-bias corrected models, we use the return time of the event in the observations as the event definition and not the observed magnitude. This gives better results than just bias-correcting the mean for the very non-linear distributions considered here.

EC-Earth

Similar to as in the observations we fit a GEV to the 16 member ensemble of the 1947-2018 simulations of the coupled model (details below). TG3x of the France averaged fitted against the modelled smoothed western European summer temperature evaluated for a 30-year return period gives a PR of 28 (17...130) and an increase in temperature ΔT = 1.7 (1.5...1.9) ºC. For the grid-point closest to Toulouse, we find PR = 100 (40...3000) and ΔT = 2.2 (2.0...2.5) ºC. Note that the curves in Fig. 12 are much more curved than in the corresponding plots of the observations due to the more negative shape parameter.

.

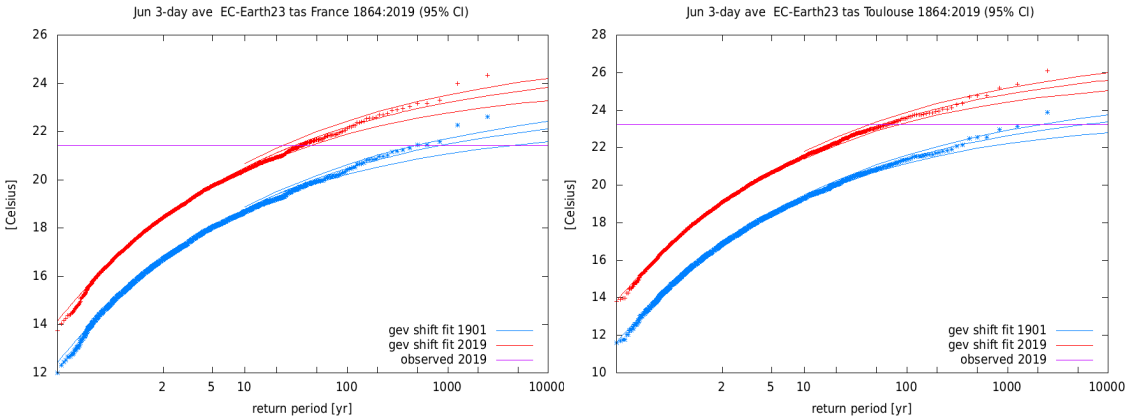

Figure 13: *Fit to highest 3-dy mean daily mean temperature averaged over France (left) and Toulouse (right) in June as described in the text for the EC-Earth ensemble. The red lines indicate the current climate, the blue ones the climate of around 1960. The purple lines indicate the 2019 value (not included in the fits).*

RACMO

Is a regional climate model dynamically downscaling the EC-Earth simulations. The RACMO simulations are analysed in exactly the same way as EC-Earth. For France we get a PR of 6.5 (4...15) and ΔT = 1.1 (0.9 1.5) ºC relative to 1960. For Toulouse the values have larger uncertainties but are otherwise compatible, PR = 8 (5 1000) and T = 1.3 (1.0 1.7) ºC relative to 1960. All these values have been extrapolated to values relative to 1900 using

the realised GMST increase up to 1960 to compare them with the other models in the synthesis section.

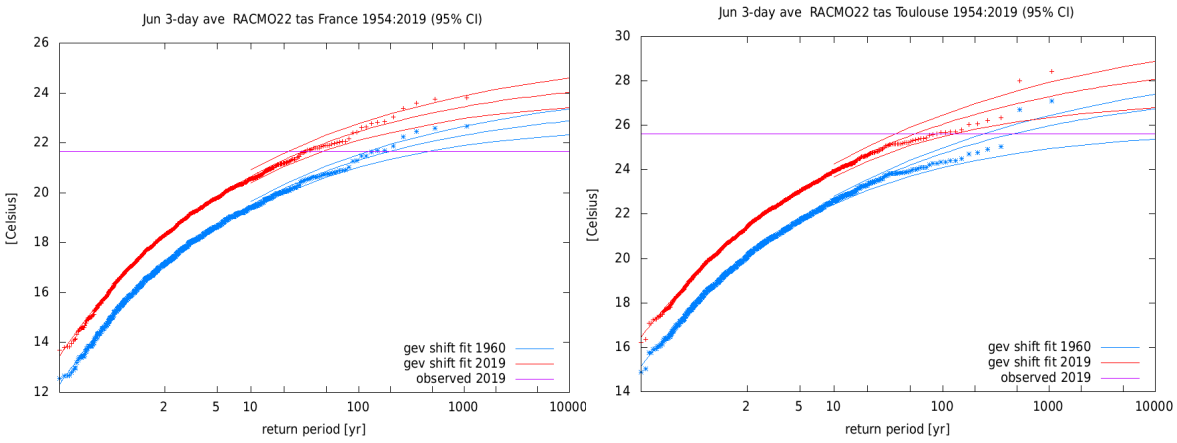

Figure 14: *Fit to highest 3-dy mean daily mean temperature averaged over France (left) and Toulouse (right) in June as described in the text for the RACMO ensemble. The red lines indicate the current climate, the blue ones the climate of around 1960. The purple lines indicate the 2019 value (not included in the fits).*

HadGEM3-A

In the same way as for EC-Earth we analyse the atmosphere-only model HadGEM3-A In this model only simulations up to the year 2015 are available.

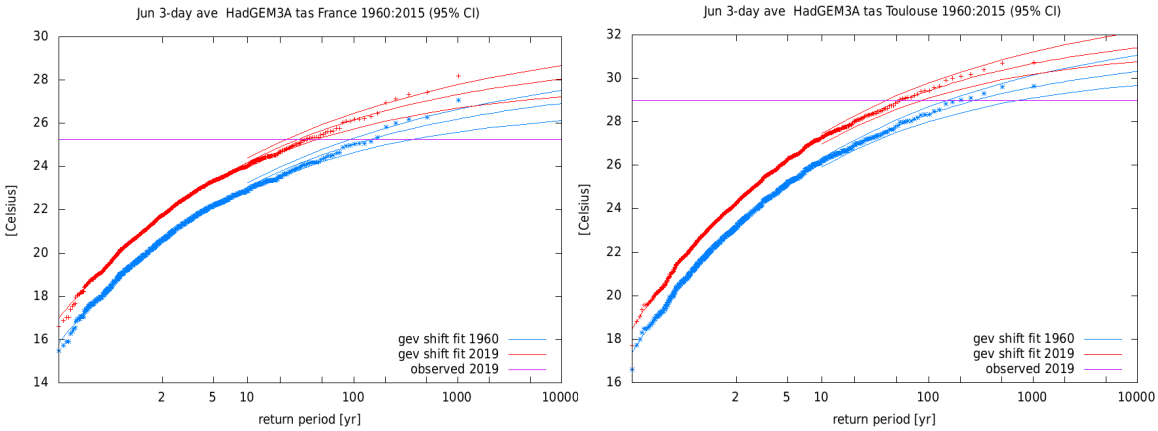

Figure 15: *Fit to highest 3-dy mean daily mean temperature averaged over France (left) and Toulouse (right) in June as described in the text for the HadGEM3-A ensemble. The red lines indicate the current climate, the blue ones the climate of around 1979. The purple lines indicate the 2019 value (not included in the fits).*

CMIP5-ETHZ

The bias-corrected CMIP5 ensemble was fitted with each ensemble member using its own smoothed western Europe summer temperature. Although the properties of the models in this ensemble differ greatly, the result after bias correction is described well by a GEV

function. The fit gives a PR of 46 (19 to 22) and a ΔT of 2.2 (1.7 to 2.2) ºC for the France average and PR = 140 (>50) for Toulouse.

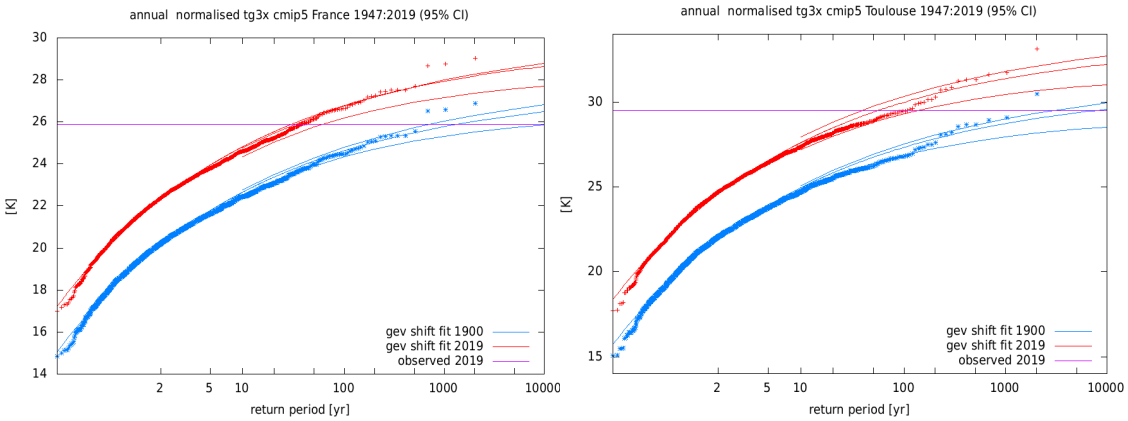

Figure 16: *Fit to highest 3-dy mean daily mean temperature averaged over France (left) and Toulouse (right) in June as described in the text for the CMIP5 ensemble. The red lines indicate the current climate, the blue ones the climate of around 1900. The purple lines indicate the 2019 value (not included in the fits).*

Weather@home

Due to the large ensemble size in weather@home we do not fit a distribution for the attribution analysis using this model but evaluate the change in probability and magnitude for the 1 in 30-year event in the simulations of France and the 1 in 55-year event for the gridpoint nearest to Toulouse in the ensemble directly. Revealing a probability ratio of 2.06 (1.26…3.34) for France and 4(1.75…10.74) over Toulouse. The change in magnitude is rather large in this model compared to others due to the very large variability.

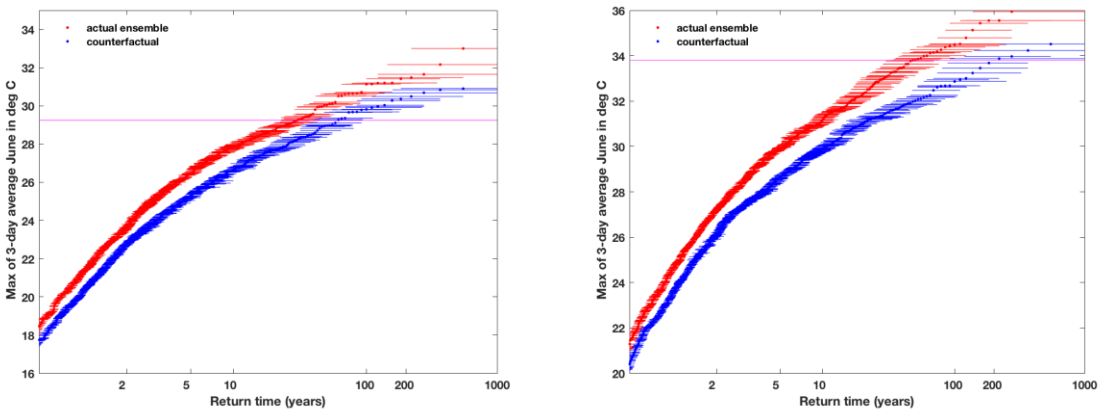

Figure 17: *Highest 3-dy mean daily mean temperature averaged over France (left) and Toulouse (right) in June as described in the text for the weather@home ensemble. The red lines indicate the current climate, the blue ones the counterfactual climate. The purple lines indicate the 2019 return-time value obtained from the observations.*

CMIP5 Météo France

An unconditional attribution is performed using the method of Ribes et al (2019). The event differs somewhat from the rest of the analysis: daily mean temperature averaged over 27-29 june, for two different spatial domains: France and Toulouse. Temperatures are assumed to follow a Gaussian law, driven by a covariate describing the climate change. The covariate is an additive fit of the mean temperature over Europe, cut in two parts : a first smooth part containing the anthropogenic signal, and the second the response to natural forcing. A multi-model synthesis of 28 CMIP5 model simulations is done, and the covariate and the stationary parameters of Gaussian law are constrained by the observations (HadCRUT4 for covariate, and Météo-France observations for parameters). All numbers and results provided below are obtained after constraining the CMIP multi-model synthesis by available observations, and are therefore a mix of these two sources of data.

The result of this procedure is given in Fig. UA-1 for all France, and UA-2 on Toulouse (France). Until the mid 70's, no significant change is detected (the confidence interval contains the value 1 for RR), then a fast increase in RR is observed. At the date of the event (2019), the risk ratio is increased by a factor 34 (5-550) for France, and the change in intensity is 1.7°C (0.8-2.6°C). For Toulouse the probability ratio is 38 (7 to 750) and the increase in temperature 1.9 °C (1.0 to 2.8 °C).

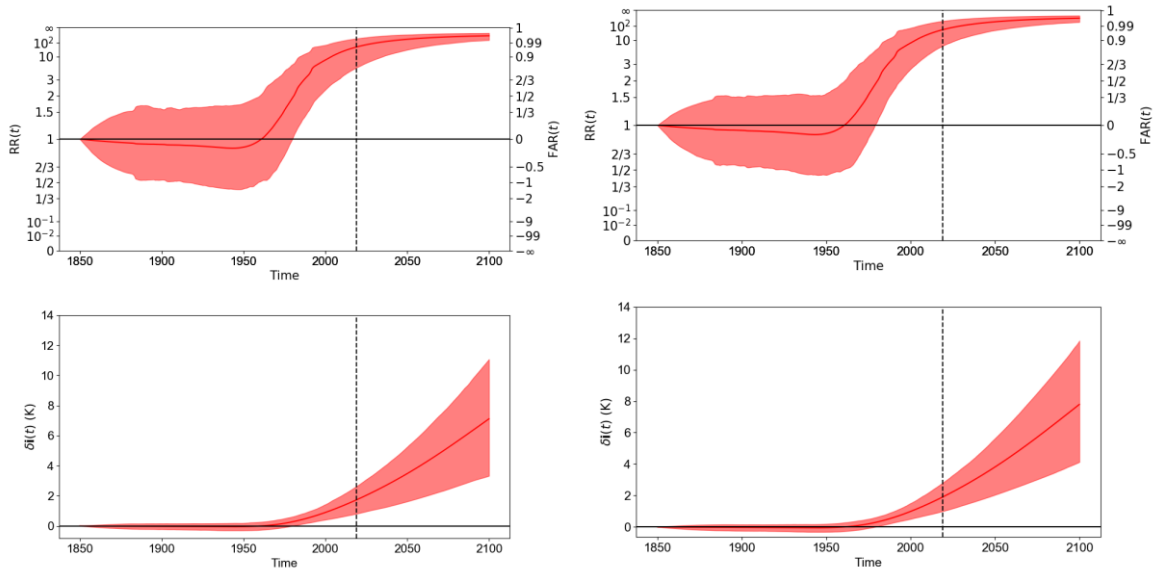

Fig. 18. Left: Risk Ratio (upper) and change in intensity (lower) for France (left) and Tououse (right). The red line is the best estimate, the red filled contour is the 95% confidence interval. The dotted black line indicate the date of the event (2019).

IPSL-CM6A-LR:

We used the 31-member ensemble of the CMIP6 IPSL-CM6A-LR historical (1850-2014) simulations prolonged to 2029 with SSP585 radiative forcings (except for constant 2014 aerosol forcing) to assess the difference between current climate (taken here as the 2005-2029 period) and a counterfactual climate, taken here as the 1850-1879 period. The ensemble has 31 members so for each tie slice there are 930 years available. We find that for this model ensemble, for France, PR=5 [2-20], and for Toulouse PR=15 [8-40].

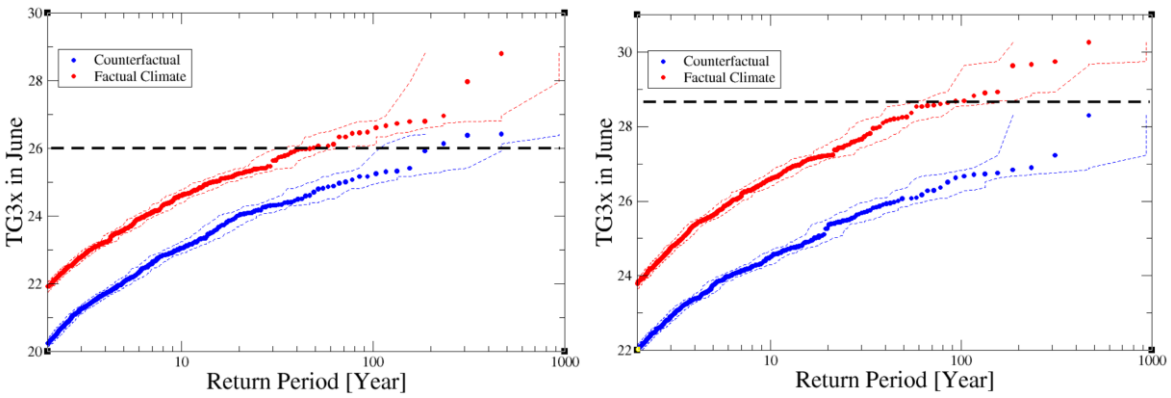

a) b)

Figure 19: (a) Return values as a function of the return period for the factual and counterfactual periods for IPSL-CM6A-LR model ensemble for the France index. (b) Probability ratio as a function of the threshold return value, showing PR=5 (2 to 20). (c) and (d): same as a) and b) for the Toulouse index. In this case PR~15 (8-40).

EURO-CORDEX

Here, the attribution is made using the 1971-2000 as a counterfactual period and 2001-2030 as a factual current period (see above). Results are plotted in Figure 19. We find, for the France index, between 1971-2000 and 2001-2030, PR=8 [3-15], and for Toulouse, PR=6 [2-20] relative to about 1985. In the synthesis these values have been scaled in inverse proportion to the global mean surface temperature change 1985-2019 to the whole 1900-2019 increase.

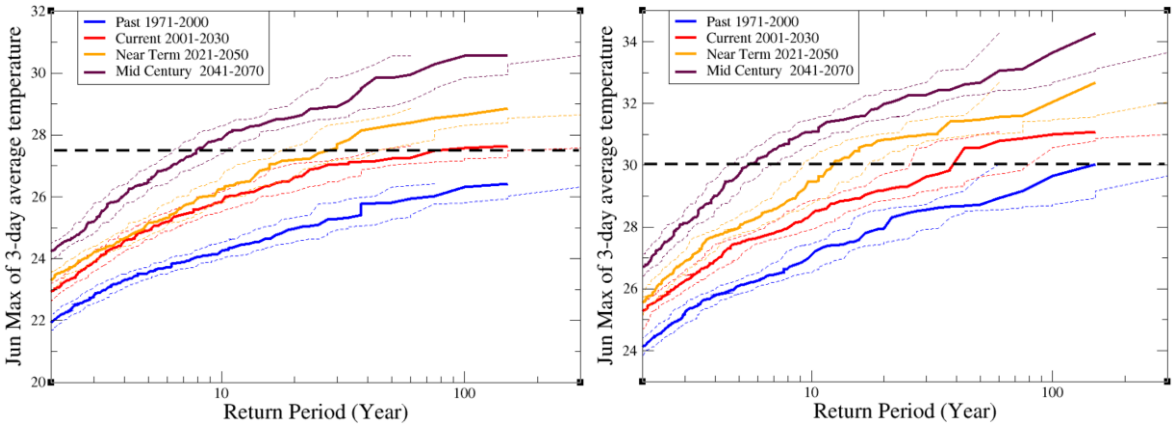

a) France (30 stations) b) Toulouse

Figure 20: Return values vs. return period in 4 time slices (late 20th century, current, near future and mid 21st century) of the pooled EURO-CORDEX ensemble of 11 GCM-RCM models. Dashed lines indicate the 5-95% confidence interval and the heavy line the median estimate from the bootstrap method.

Hazard synthesis

We summarise the results from the observations and the climate models, answering the questions how much the probability and severity of an event like this (or more severe) have changed due to anthropogenic climate change.

The change in probability (Probability Ratio, PR) is shown in figure 21. First and foremost, the observations and almost all models show a large increase in the probability of heat waves like the one observed in June 2019 (as described by the 3-day mean temperature, both averaged over all of France and in one specific city, Toulouse).

For the average over France we find that the probability has increased by *at least* a factor five (excluding the model with very strong bias in variability). However, the observations show it could be much higher still, a factor 100 or more. Similarly, the observed trend in temperature of the heat during an event with a similar frequency is around 4 °C, whereas the climate models show a much lower trend.

We note that while we are very confident about the positive trend and the fact that the probability has increased by *at least* a factor five, it is much more difficult to assign one specific number (a “best guess” based on all models and observations) on the extent of the increase, given the large uncertainties in the observed trends (due to the relatively short time series from 1947-2019) and systematic differences between the representation of extreme heat waves in the climate models and in the observations.

For one city, Toulouse, the results are very similar although with somewhat larger uncertainties.

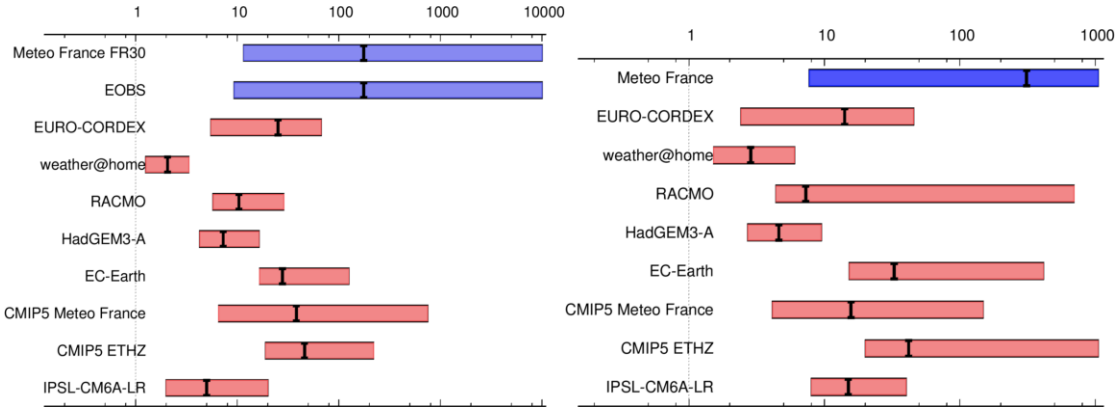

Figure 21. Left: Increase in probability for a the highest 3-day mean temperature averaged over France. Blue: observations. red: climate models. Right: same for Toulouse. Note that the climate models have systematic biases in their representation of heat waves.

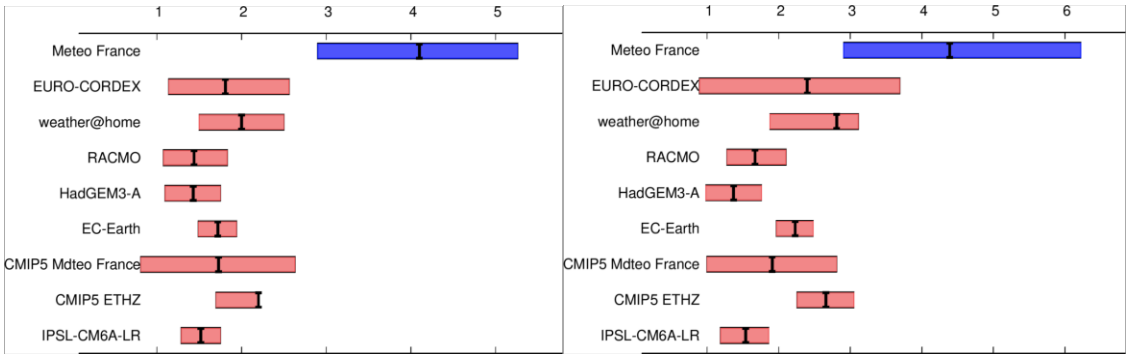

Figure 22. The increase in temperature is shown in figure above, left for the average over France, right for Toulouse. There is no overlap between the trend in the *observations, around 4 ºC , and the modelled trends, around 2 ºC.*

Vulnerability and Exposure

Immediate impacts of the heat wave were reported extensively in national and international media. However, the most striking impact, mortality due to a variety of causes aggravated by the extreme heat, is generally only reported later (with the exception of immediate deaths such as due to drowning when people seek cooling). This “excess mortality” beyond the normal mortality in this period of the year (and often taking account of reduced mortality in the following weeks) is calculated on statistical analysis of reported deaths over a longer period of time. This generally means that heat wave mortality, while very significant compared to other disasters in terms of numbers

of people killed, often attracts much less public attention that, for instance, deaths due to floods or storms. This is despite the fact that climate change is bringing substantial increases in the number of days globally when heat-related deaths are expected to occur (Christidis et al, 2019).

In 2003, an extreme heat wave in August resulted in tens of thousands of deaths, and dramatic national concern about the lack of preparedness. This heat wave was one of the first explicitly attributed to climate change; Stott et al. (2004) found very likely at least a doubling of the frequency of such events. However, it is also frequently used, including by the IPCC, as an example of rising risks due to a combination of rising climate hazards and increasing exposure and vulnerability, in this case due to an aging population, urbanisation and changing social structures (more elderly people living alone) (e.g. Murray et al. 2012). In general, the elderly, chronically ill and very young tend to be the most vulnerable to heat waves.

Since 2003, significant measures have been put in place in France to reduce the impacts of heat waves, in particular through the “Plan Canicule”. In June 2019, heat wave warnings were activated all around the country, including specific measures taken by public authorities, but also strong behavioral advice to the general population. Some studies (e.g Fouillet et al. 2008) have suggested a significant decrease in relative mortality due to such measures in the years since 2003. Others however (e.g. Pascal et al. 2019), show less differences in heat wave mortality before and after 2003, and indicate, in any case, that there is still significant avoidable mortality associated with heat waves. In the context of the current heat wave, impacts are likely to be especially pronounced given that the heat occurred so early in the summer, when people are not less accustomed to the heat. However, impacts on other systems, such as power generation, may be less pronounced given that cooling water is likely still more readily available than later in the summer. Significant impacts were also reported on the risk of fires (with significant fires especially in Spain) and on agricultural production (where of course the timing of the heat also affects impacts on various types of crops differently).

In summary, changes in frequency, intensity but also timing of heat waves hazards can have significant impacts on mortality and other risks, yet they combine with other risk drivers related to the vulnerability and exposure of the affected population. The impact on mortality will only become apparent some time after the event.

Appendix: model details:

EURO-CORDEX: we use here an ensemble of 11 GCM-RCM models that were also used in previous studies for heat waves, heavy precipitation and storms (see eg. Kew et al., 2018; Luu et al., 2019; Vautard et al., 2019). These models were bias-adjusted using the CDFt method (Vrac et al., 2016) using a methodology that was deployed for serving the energy sector within the Copernicus Climate Change Service (Bartok et al., submitted to Climate Services).

CMIP5 global climate model simulations: We use here single runs (r1i1p1) of 28 model simulations from the 5th phase of the Coupled Modeling Intercomparison Project (CMIP5; Taylor, et.al. 2012) for historical and future simulations under a high emission scenario (RCP8.5, van Vuuren et al. 2011); see Table 2) building upon previous analyses with these data (e.g. Vogel et al. 2019). We compute TG3x between 1870-2100 from daily air temperatures (*tas* in CMIP5) for each model in the original resolution and then average over metropolitan France and Toulouse. For the covariate we compute mean summer temperatures on land over Western European (35°N-72N, 15°W-20°E).
All temperatures from the CMIP5 ensemble simulations are bias corrected to E-OBS (Haylock et al. 2008) temperatures for the reference period 1950-1979 for each model individually. To fit GEVs we pool the data from the whole CMIP5 ensemble from 1947-2018 which allows a robust estimate.

Table 2. Overview of 28 CMIP5 models used in this study. For each model we use one ensemble member from the historical period and RCP8.5.

Model name	Modeling center
ACCESS1.0	Commonwealth Scientific and Industrial Research Organization (CSIRO) and Bureau of Meteorology (BOM), Australia\
ACCESS1.3	Commonwealth Scientific and Industrial Research Organization (CSIRO) and Bureau of Meteorology (BOM), Australia\\
BCC-CSM1.1	Beijing Climate Center, China Meteorological Administration
BCC-CSM1.1M	Beijing Climate Center, China Meteorological Administration

CanESM2	Canadian Centre for Climate Modelling and Analysis
CCSM4	National Center for Atmospheric Research
CESM1(BGC)	Community Earth System Model Contributors
CMCC-CESM	Centro Euro-Mediterraneo sui Cambiamenti Climatic
CMCC-CM	Centro Euro-Mediterraneo sui Cambiamenti Climatici
CMCC-CMs	Centro Euro-Mediterraneo sui Cambiamenti Climatici
CNRM-CM5	Centre National de Recherches Météorologiques / Centre Européen de Recherche et Formation Avancée en Calcul Scientifique\\
CSIRO-Mk3.6.0	Commonwealth Scientific and Industrial Research Organization in collaboration with Queensland Climate Change Centre of Excellence
EC-EARTH	European-Earth-System-Model Consortium
GFDL-CM3	NOAA Geophysical Fluid Dynamics Laboratory
HadGEM2-A0	Met Office Hadley Centre
HadGEM2-CC	Met Office Hadley Centre
INM-CM4	Institute for Numerical Mathematics
IPSL-CM5A-LR	Institut Pierre-Simon Laplace

IPSL-CM5A-MR	Institut Pierre-Simon Laplace
IPSL-CM5B-LR	Institut Pierre-Simon Laplace
MIROC-ESM	Japan Agency for Marine-Earth Science and Technology, Atmosphere and Ocean Research Institute (The University of Tokyo), and National Institute for Environmental Studies
MIROC-ESM-CHEM	Japan Agency for Marine-Earth Science and Technology, Atmosphere and Ocean Research Institute (The University of Tokyo), and National Institute for Environmental Studies\\
MIROC5	Atmosphere and Ocean Research Institute (The University of Tokyo), National Institute for Environmental Studies, and Japan Agency for Marine-Earth Science and Technology \\
MPI-ESM-LR	Max-Planck-Institute for Meteorology
MPI-ESM-MR	Max-Planck-Institute for Meteorology
MRI-CGCM3	Meteorological Research Institute
MRI-ESM1	Meteorological Research Institute
NorESM1-M	Norwegian Climate Centre\

RACMO 2.2: this regional climate model ensemble downscales 16 initial-condition realizations of the EC-EARTH 2.3 coupled climate model in the CMIP5 RCP8.5 scenario

(Lenderink et al., 2014; Aalbers et al., 2017) on a smaller European domain over 1950-2100.

HadGEM3-A-N216: the atmosphere-only version of the Hadley Centre climate model. For the trend analysis we use the 15 members run for the EUCLEIA project 1961-2015.

EC-Earth 2.3: a coupled GCM, 16 members using historical/RCP8.5 forcing over 1861-2100 (Hazeleger et al, 2010), each producing a transient climate simulation from 1860 to 2100. The model resolution is T159 which translates to around 150 km in the European domain. The underlying scenarios are the historical CMIP5 protocols until the year 2005 and the RCP8.5 scenario (Taylor et al. 2012) from 2006 onwards. Up to about 2030, the historical and RCP8.5 temperature evolution is very similar.

RACMO is a regional climate model developed at KNMI. An ensemble of sixteen members was generated to downscale the above-mentioned EC-Earth experiments over the period 1950-2100 at a resolution of about 11km (Lenderink et al., 2014, Aalbers et al., 2018).

The 15 HadGEM3-A atmosphere-only runs from 1960–2015 (Ciavarella et al, 2017) (N216, about 60km) are evaluated for the separate regions. The model is driven by observed forcings and sea-surface temperatures (SSTs) ("historical") and with preindustrial forcings and SSTs from which the effect of climate change has been subtracted ("historicalNat"). The latter change has been estimated from the Coupled Model Intercomparison Project phase 5 (CMIP5) ensemble of coupled climate simulations.

Weather@home: Using the distributed computing framework known as weather@home (Guillod et al., 2017, Massey et al., 2015) we simulate two different large ensembles of June and July weather, using the Met Office Hadley Centre regional climate model HadRM3P at 25km resolution over Europe embedded in the atmosphere-only global circulation model HadAM3P. The first set of ensembles represents possible weather under current climate conditions (prescribed OSTIA sea surface temperatures for 2006-2015). This ensemble is called the "all forcings" scenario and includes human-caused climate change. The second set of ensembles represents possible summer weather in a world as it might have been without anthropogenic climate drivers. This ensemble is called

the “natural” or “counterfactual” scenario with prescribed sea surface temperatures obtained from CMIP5 simulations (Schaller et al., 2016).

IPSL-CM6A-LR is the latest version of the IPSL climate model which was prepared for CMIP6 (publications in preparation, Servonnat et al., 2019; Lurton et al., 2019). It couples the LMDZv6 atmospheric model, the NEMO ocean, sea ice and marine biogeochemistry model and the ORCHIDEE land surface model. The resolution of the atmospheric model is 144x143 points in longitude and latitude, which corresponds to an average resolution of 160 km, and 79 vertical layers. The resolution of the ocean model is 1°x1° and 75 layers in the vertical. An ensemble of 31 historical simulations have been run for CMIP6 for the period 1850-2014 and have been prolonged until 2029 with SSP585 radiative forcings (except for constant 2014 aerosol forcing). LMDZv6 includes a ``New Physics'' package based on a full rethinking of the parametrizations of turbulence, convection and clouds on which the IPSL-CM6A-LR climate model is built.

References

Bartok, B., M. Wild, D. Folini, D. Luethi, S. Kotlarski, C. Schär, R. Vautard, S. Jerez, and Z. Imecs (2017) Projected changes in surface solar radiation in CMIP5 global climate models and in EURO-CORDEX regional climate models for Europe. Climate Dynamics, DOI 10.1007/s00382-016-3471-2.

Christidis N, Jones GS, Stott PA. (2015) Dramatically increasing chance of extremely hot summers since the 2003 European heatwave, Nature Climate Change, 5, 1, 46-50, DOI:10.1038/NCLIMATE2468.

Christidis, N., Mitchell, D., Stott, P. A. (2019) Anthropogenic climate change and heat effects on health. International Journal of Climatology, doi:10.1002/joc.6104.

D'Ippolita, D. et al (2010) The impact of heat waves on mortality in 9 European cities: results from the EuroHEAT project. Environmental Health 9, 37. doi:10.1186/1476-069X-9-37

Haylock, M. R., Hofstra, N., Klein Tank, A. M. G., Klok, E. J., Jones, P. D., and New, M. (2008) A European daily high-resolution gridded data set of surface temperature and precipitation for 1950–2006, J. Geophys. Res., 113, D20119, https://doi.org/10.1029/2008JD010201.

IPCC, 2012: Managing the Risks of Extreme Events and Disasters to Advance Climate Change Adaptation. [Field, C.B., V. Barros, T.F. Stocker, D. Qin, D.J. Dokken, K.L. Ebi, M.D. Mastrandrea, K.J. Mach, G.-K. Plattner, S.K. Allen, M. Tignor, and P.M. Midgley (eds.)]. A Special Report of Working Groups I and II of IPCC Intergovernmental Panel on Climate Change. Cambridge University Press, Cambridge, United Kingdom and New York, USA, 594 pp.

IPCC, 2013: Climate Change 2013: The Physical Science Basis. Working Group I Contribution to the Fifth Assessment Report of the Intergovernmental Panel on Climate Change. [Stocker, T.F., D. Qin, G.-K. Plattner, M. Tignor, S.K. Allen, J. Boschung, A. Nauels, Y. Xia, V. Bex, and P.M. Midgley (eds.)]. Cambridge University Press, Cambridge, United Kingdom and New York, NY, USA, 1535 pp

IPCC, 2018: Summary for Policymakers. In: Global warming of 1.5°C. An IPCC Special Report on the impacts of global warming of 1.5°C above pre-industrial levels and related global greenhouse gas emission pathways, in the context of strengthening the global response to the threat of climate change, sustainable development, and efforts to eradicate poverty [V. Masson-Delmotte, P. Zhai, H. O. P.rtner, D. Roberts, J. Skea, P. R. Shukla, A. Pirani, W. Moufouma-Okia, C. P.an, R. Pidcock, S. Connors, J. B. R. Matthews, Y. Chen, X. Zhou, M. I. Gomis, E. Lonnoy, T. Maycock, M. Tignor, T. Waterfield (eds.)]. World Meteorological Organization, Geneva, Switzerland, 32 pp.

Kew, S. et al, (2019) The exceptional summer heatwave in Southern {Europe} 2017. Bull. Amer. Met. Soc., 100, S2-S5. doi:10.1175/BAMS-D-18-0109.1

Mueller, B. and S.I. Seneviratne (2012) Hot days induced by precipitation deficits at the global scale. Proceedings of the National Academy of Sciences, 109(31), 12398–12403, doi:10.1073/pnas.1204330109.

Seneviratne S.I., T. Corti, E.L. Davin, M. Hirschi, E.B. Jaeger, I. Lehner, B. Orlowsky and A.J. Teuling (2010) Investigating soil moisture-climate interactions in a changing climate: A review. Earth Sci. Rev., 99,125–161.

Sippel, S., J. Zscheischler, M.D. Mahecha, R. Orth, M. Reichstein, M. Vogel, and S.I. Seneviratne (2017) Refining multi-model projections of temperature extremes by evaluation against land–atmosphere coupling diagnostics. Earth System Dynamics, 8, 387–403, 2017 www.earth-syst-dynam.net/8/387/2017/ doi:10.5194/esd-8-387-2017

Stott PA, Stone DA, Allen MR. (2004) Human contribution to the European heatwave of 2003, Nature, 432, 7017, 610-614, DOI:10.1038/nature03089.

Taylor, K. E., R. J. Stouffer, and G. A. Meehl (2012) An overview of CMIP5 and the experiment design, Bull. Am. Meteorol. Soc., 93(4), 485–498.

van Vuuren, D.P., Edmonds, J., Kainuma, M. et al. Climatic Change (2011) 109, 5. https://doi.org/10.1007/s10584-011-0148-z

Vautard, R. et al (2018) Evaluation of the HadGEM3-A simulations in view of climate and weather event human influence attribution in Europe. Clim. Dyn. 52 1187–1210. doi:10.1007/s00382-018-4183-6

Vogel M.M., J. Zscheischler, R. Wartenburger, D. Dee, and S.I. Seneviratne (2019, accepted). Concurrent 2018 hot extremes across Northern Hemisphere due to human-induced climate change. Earth's Future, accepted.

Wild, M. (2009) Global dimming and brightening: A review. J. Geophys. Res., vol. 114, D00D16, doi:10.1029/2008JD011470, 2009